

RESEARCH ARTICLE

Open Access



# GhPME36 aggravates susceptibility to *Liriomyza sativae* by affecting cell wall biosynthesis in cotton leaves

Zheng Yang<sup>1,3†</sup>, Menglei Wang<sup>1†</sup>, Senmiao Fan<sup>2,6</sup>, Zhen Zhang<sup>2</sup>, Doudou Zhang<sup>1</sup>, Jie He<sup>1</sup>, Tongyi Li<sup>1</sup>, Renhui Wei<sup>2</sup>, Panpan Wang<sup>1</sup>, Muhammad Dawood<sup>4</sup>, Weijie Li<sup>2</sup>, Lin Wang<sup>2</sup>, Shaogan Wang<sup>2</sup>, Youlu Yuan<sup>1,2\*</sup> and Haihong Shang<sup>1,2,5\*</sup> 

## Abstract

**Background** Cotton is an important economic crop and a host of *Liriomyza sativae*. Pectin methylesterase (PME)-mediated pectin metabolism plays an indispensable role in multiple biological processes *in planta*. However, the pleiotropic functions of PME often lead to unpredictable effects on crop resistance to pests. Additionally, whether and how PME affects susceptibility to *Liriomyza sativae* remain unclear.

**Results** Here, we isolated GhPME36, which is located in the cell wall, from upland cotton (*Gossypium hirsutum* L.). Interestingly, the overexpression of GhPME36 in cotton caused severe susceptibility to *Liriomyza sativae* but increased leaf biomass in Arabidopsis. Cytological observations revealed that the cell wall was thinner with more demethyl-esterified pectins in GhPME36-OE cotton leaves than in WT leaves, whereas the soluble sugar content of GhPME36-OE cotton leaf cell walls was accordingly higher; both factors attracted *Liriomyza sativae* to feed on GhPME36-OE cotton leaves. Metabolomic analysis demonstrated that glucose was significantly differentially accumulated. Transcriptomic analysis further revealed DEGs enriched in glucose metabolic pathways when GhPME36 was overexpressed, suggesting that GhPME36 aggravates susceptibility to *Liriomyza sativae* by affecting both the structure and components of cell wall biosynthesis. Moreover, GhPME36 interacts with another pectin-modifying enzyme, GhC/VIF1, to maintain the dynamic stability of pectin methyl esterification.

**Conclusions** Taken together, our results reveal the cytological and molecular mechanisms by which GhPME36 aggravates susceptibility to *Liriomyza sativae*. This study broadens the knowledge of PME function and provides new insights into plant resistance to pests and the safety of genetically modified plants.

**Keywords** PME, Cotton, *Liriomyza sativae*, Cell wall biosynthesis, Glucose metabolism

<sup>†</sup>Zheng Yang and Menglei Wang contributed equally to this work.

\*Correspondence:

Youlu Yuan

yuanyoulu@caas.cn

Haihong Shang

shanghaihong@caas.cn

Full list of author information is available at the end of the article



## Background

Cotton is an important source of natural fiber and is planted worldwide [1]. There is a long history and solid foundation in the transgenic technology of insect-resistant cotton varieties [2]. *Liriomyza sativae* (leaf miner), a member of *Agromyzidae*, is a widely distributed herbivorous insect that infects more than 60 host plants belonging to 18 different families [3]. Larvae of the leaf miner burrow into the leaf matter and feed on mesophyll tissue, gradually causing the leaves to yellow and ultimately wither away. In this process, chlorophyll and sugars are degraded in mesophyll cells, causing the shedding of leaves [4], which significantly reduces the production of vegetables and food crops worldwide [5]. New damage areas and new leaf miner host plants have been reported continuously over recent years [6–8]. It has been listed as a quarantine object in Europe, China, and other countries and regions [3, 9]. As a member of the Malvaceae family, cotton is a potential leaf miner host, which qualifies it as a suitable receptor material for studying the mechanism of susceptibility to leaf miners. Currently, the common control methods for leaf miner include space isolation, insecticide use, breeding of resistant plants, and biological control. However, most insecticides have gradually become less effective. After the release of parasitic bees, the natural enemies of leaf miner, other organisms of plants were also attacked [3]. Owing to the fast propagation capability of leaf miners, strict quarantine examination is still regarded as a necessary means to prevent their spread and outbreak.

The function of plant cells depends on their morphological characteristics and components [10]. The cell wall is the extracellular matrix of plants, whose chemical structure and mechanical properties play important roles in determining cell shape and development. Cell wall loosening and rigidification are important factors that determine the anisotropic growth mode and shape of plant cells [11]. Additionally, the cell wall is a medium for interactions between cells and the external environment [12–14]. The role of the cell wall in coping with biological stress [15, 16] and abiotic stress [17, 18] has received increasing attention. Pectin, an important cell wall polysaccharide, is the most abundant biomolecule in the primary wall, accounting for approximately one third of its dry weight [19]. It is involved in cell adhesion and separation [20] and helps maintain cell integrity [21]. Pectin is synthesized in the Golgi apparatus in a state of high methyl esterification [22] and is then secreted from cells [23]. It forms a crosslinking network with cellulose and hemicellulose [24], which constitutes the main component of the cell wall.

Pectin is modified by pectin methylesterase (PME, EC 3.1.1.11), causing a decrease in pectin

methylesterification [25]. Pectin demethylesterification leads the cell wall to two contrasting fates, harder or softer, depending on the environment of the early developmental stage: in an environment where divalent cations such as  $\text{Ca}^{2+}$  are present, pectin methylated at low levels forms a harder structure with other homogalacturonan (HG) molecules; in an environment containing polygalacturonase, pectin methylated at low levels disintegrates as a target, and the cell wall become softer [26]. The changes in cell wall hardness caused by pectin demethylesterification have already been verified in pollen tubes and onion epidermis [27, 28]. The results of an in vitro study also confirmed the role of pectin demethylesterification in stabilizing the cellulose network [29]. Moreover, the presence of cellulose also has a positive effect on pectin demethylesterification [30].

PME is a key enzyme of pectin metabolism that is widely found in higher plants and is encoded by a polygene family [31, 32]. PME can be divided into two types according to protein structure: type I contains pectin methylesterase inhibitor (PMEI) and PME domains, whereas type II possesses only PME domains [33]. PME is involved in important physiological processes related to the vegetative growth and reproductive development of plants through the metabolism of cell wall pectin, such as fruit ripening and softening [34], stomatal opening and closing [35], seed mucus secretion [36], and pollen tube growth [37]. Previous studies indicate that the modification of pectin by PME plays an important role in plant growth and development. The knockout, overexpression, and heterologous expression of *PME* genes in *Arabidopsis* lead to significant changes in the plant phenotype, such as decreased stem mechanical strength [38], an altered number of adventitious roots [39], improved salt tolerance [40], decreased plant height [41], and decreased photosynthetic efficiency [42].

The effect of the PMEI on PME activity has been extensively analyzed [43]. PMEI and PME combine into a nonspecific complex in a 1:1 ratio [44], which prevents pectin from being demethylated by inhibiting the combination of PME and its target. The interaction between the PME and PMEI influences the degree of pectin methylesterification and subsequently affects in plant seed germination, pollen tube development, root development, and stress responses [45]. Additionally, pectin methylesterification plays important role in plant resistance to diseases [46, 47] and pests [15]. For example, constitutive overexpression of *AtPMEI-1* and *AtPMEI-2* in *Arabidopsis* increases the degree of pectin methylesterification to restrict fungal infection by *Botrytis cinerea* [48]. Pectin methyl esterase 1 reduces the degree of esterification of pectin-derived oligogalacturonides to elicit defense responses in strawberry [49].

Methanol (MeOH), a byproduct of HG demethylesterification, is regarded as a signal of plant immunity [50]. And the PME activity of host plants is positively correlated with the feeding preference of aphids [15].

To explore the function of pectin methylesterification in upland cotton, we previously explored the phylogeny and expression of the PME gene family [33]. Here, GhPME36 was used as the research subject. By knocking out and overexpressing GhPME36, we surprisingly revealed the relationship between pectin methylesterification and the susceptibility of upland cotton to leaf miners. Cytological, transcriptomic, and metabolomic analyses revealed that the increased glucose level and looser cell wall structure of GhPME36-overexpressing (GhPME36-OE) cotton leaves resulted in greater susceptibility to leaf miners. This study lays a foundation for the breeding of insect-resistant cotton genotypes by providing a new idea for resistance to *Liriomyza sativae*.

## Results

### Expression pattern and subcellular localization of GhPME36

Compared with that in other organs and tissues, the expression of GhPME36 was relatively low in the leaves, as indicated by the published transcriptome data (Additional file 1: Fig. S1). To understand the role of GhPME36 in cotton leaves, the expression of GhPME36 was determined in leaves at 7, 14, 21, 28, and 35 days after leaf spreading (D). The highest expression level of GhPME36 was observed at 7 D. With the development of cotton leaves, the expression of GhPME36 decreased tenfold until 28 D and then increased sharply at 35 D, when the leaves had almost matured (Fig. 1A).

A subcellular localization experiment conducted on tobacco leaves revealed that GhPME36 was localized in the cell wall and/or membrane (Additional file 1: Fig. S2). For clearer research, onion inner epidermis was used as the transformation receptor. GhPME36 was verified to be located in the cell wall rather than the cell membrane

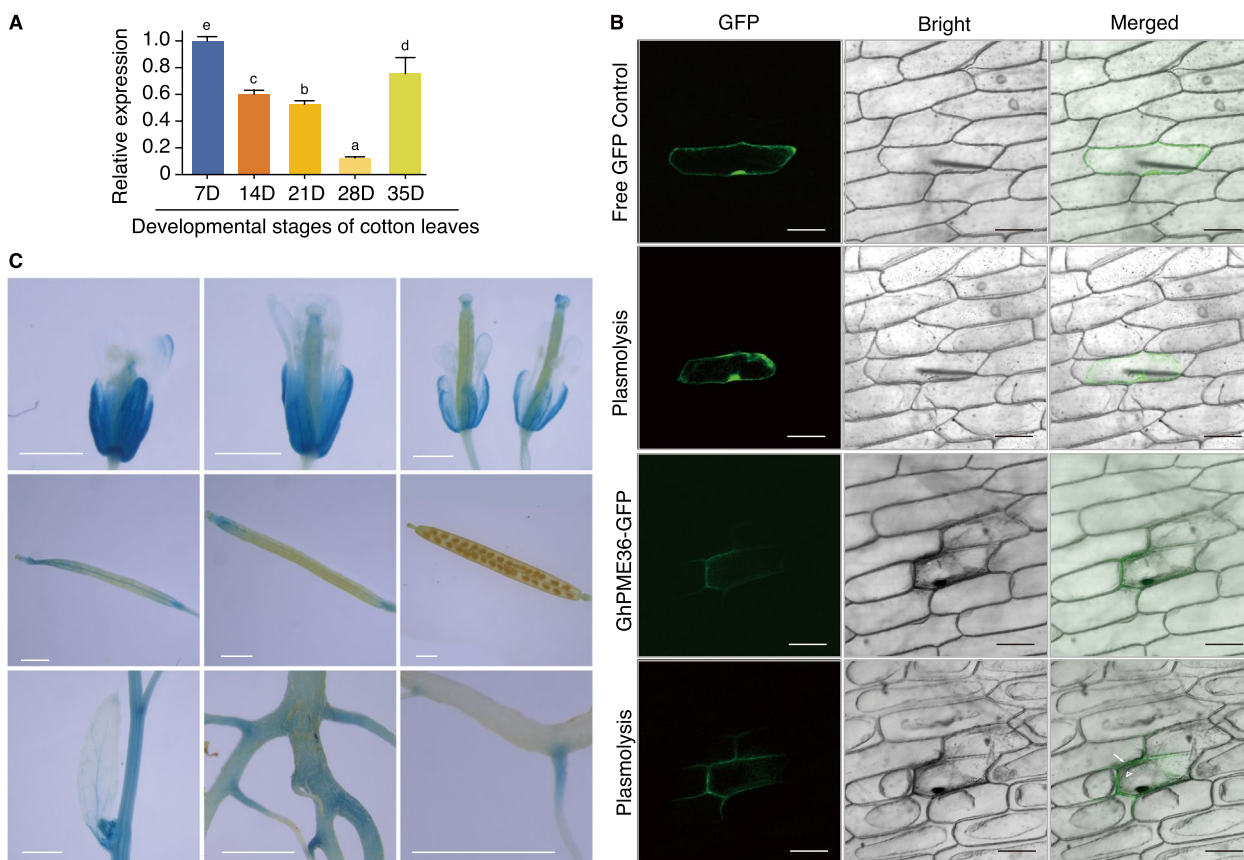


**Fig. 1** Expression pattern of GhPME36. **A** Expression level of GhPME36 during the developmental stages of upland cotton (CCRI24) leaves. The data are presented as the means  $\pm$  SDs ( $n = 3$  biological replicates). Different letters indicate significant differences ( $P < 0.05$ ; Duncan's multiple range test). **B** Subcellular localization of GhPME36 in onion epidermis. The arrow indicates the cell wall; open triangle indicates the plasma membrane. Scale bar, 100  $\mu$ m. **C** Histochemical analysis of GUS activity in the flowers, pods, leaves, stems, and roots and root hairs of proGhPME36:GUS transgenic Arabidopsis. Scale bar, 1 mm

by plasmolysis (Fig. 1B). GUS staining in *Arabidopsis* further demonstrated the expression of the *GhPME36* promoter in the calyx, pod, leaf vein, stems, and root epidermis (Fig. 1C). These results indicate the potential role of *GhPME36* in the initiation and maturation of cotton leaves and that GhPME36 might be involved in cell wall biosynthesis.

**Overexpression of GhPME36 in *Arabidopsis* increased leaf biomass**

To preliminarily understand the function of *GhPME36* in *planta*, seven *Arabidopsis* transgenic lines overexpressing *GhPME36* were generated, in which the expression level of *GhPME36* increased by nine to 125 times (Additional file 1: Fig. S3A). Compared with the wild type (WT), the overexpression of *GhPME36* clearly increased plant size (Fig. 2A) and larger rosette leaves (Fig. 2B) in three randomly selected lines.

Three weeks after sowing, the diameter of the plants was 28–46% greater when *GhPME36* was overexpressed than in the WT (Fig. 2C). Moreover, the leaf lengths

of the three *GhPME36*-OE lines were also 28%, 48%, and 32% greater, respectively (Fig. 2D). To determine the reason for the larger transgenic leaves, the rosette leaf weight was determined. The fresh weight was 60%, 111%, and 70% higher (Fig. 2E), and the dry weight was 59%, 104%, and 65% greater in the *GhPME36*-OE lines compared with the WT (Fig. 2F). Notably, for each *GhPME36*-OE line, the increasing proportion of fresh weight and dry weight was almost the same, which indicated that GhPME36 generally increased the leaf biomass by producing more dry materials.

**Overexpression of GhPME36 increased leaf miner susceptibility in cotton**

To further explore the function of *GhPME36* in cotton leaves, eight *GhPME36*-OE and seven *GhPME36*-knockout (*GhPME36*-KO) cotton plants were obtained. Three lines from each transgenic event were randomly selected for the following experiments. The expression level of *GhPME36* in three selected *GhPME36*-OE cotton lines increased by 3.2–5.9 times (Additional file 1: Fig.

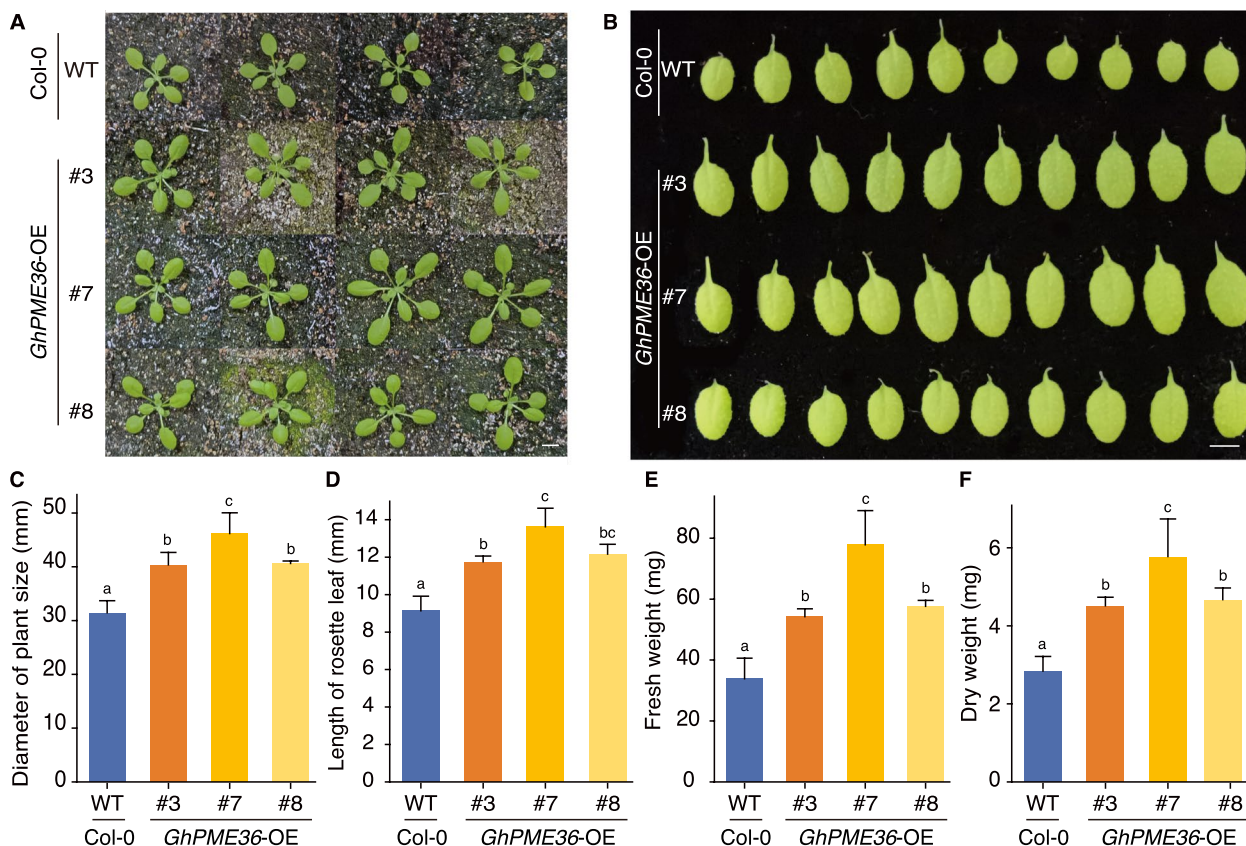


**Fig. 2** Morphology and leaf weight of *GhPME36*-OE *Arabidopsis*. **A** Phenotypes of three-week-old WT and *GhPME36*-OE *Arabidopsis* plants. Scale bar, 1 cm. **B** Phenotypes of fifth to eighth rosette leaves of WT and *GhPME36*-OE *Arabidopsis* plants. Scale bar, 1 cm. **C–F** Plant size (**C**), rosette leaf length (**D**), fresh weight (**E**), and dry weight (**F**) of WT and *GhPME36*-OE three-week-old *Arabidopsis*. The data are presented as the means  $\pm$  SDs ( $n=5$  biological replicates). Different letters indicate significant differences ( $P < 0.05$ ; Duncan’s multiple range test)

S3B). To evaluate the efficiency of the overexpression and silencing of *GhPME36*, the total PME activity in cotton leaves was determined. Compared with that in WT cotton leaves, the PME activity was significantly (16–18%) higher in *GhPME36*-OE cotton leaves (Fig. 3A) and 11–27% lower in *GhPME36*-KO cotton leaves (Fig. 3B). The effect of *GhPME36* expression on PME activity demonstrated that *GhPME36* had PME enzyme activity.

When cultivated in the field, the pest index of the *GhPME36*-OE lines was significantly (2750%) higher than that of the WT, whereas the *GhPME36*-KO lines presented distinct resistance (Fig. 3C) according to the indexing grade shown in Additional file 2: Table S1. The mature leaves of *GhPME36*-OE plants were severely attacked by the leaf miner and withered over time (Fig. 3D). These results showed that *GhPME36* distinctly increased the susceptibility of cotton leaves to leaf miners. Additionally, among these transgenic lines, *GhPME36*-OE line 3 and *GhPME36*-KO line 3 presented

the most striking differences in PME activity and were selected for further research.

**Overexpression of *GhPME36* decreased pectin methylesterification and epidermal cell wall thickness in cotton leaves**

In the *GhPME36*-OE cotton leaves, the cell walls of both the upper and lower epidermis were thinner than those of the WT plants (Fig. 4A). The most significant changes occurred in 14 D and 28 D leaves. Specifically, the cell wall thickness of the upper epidermis was 11–32% smaller (Fig. 4B), whereas that of the lower epidermis was 13–25% smaller (Fig. 4C) than that of the WT. As for *GhPME36*-KO cotton leaves, the cell wall thickness of upper epidermis significantly increased by 8.9% compared with that of the WT. However, the lower epidermal cell wall thickness of WT and *GhPME36*-KO cotton leaves showed no obvious difference (Additional file 1: Fig. S4).

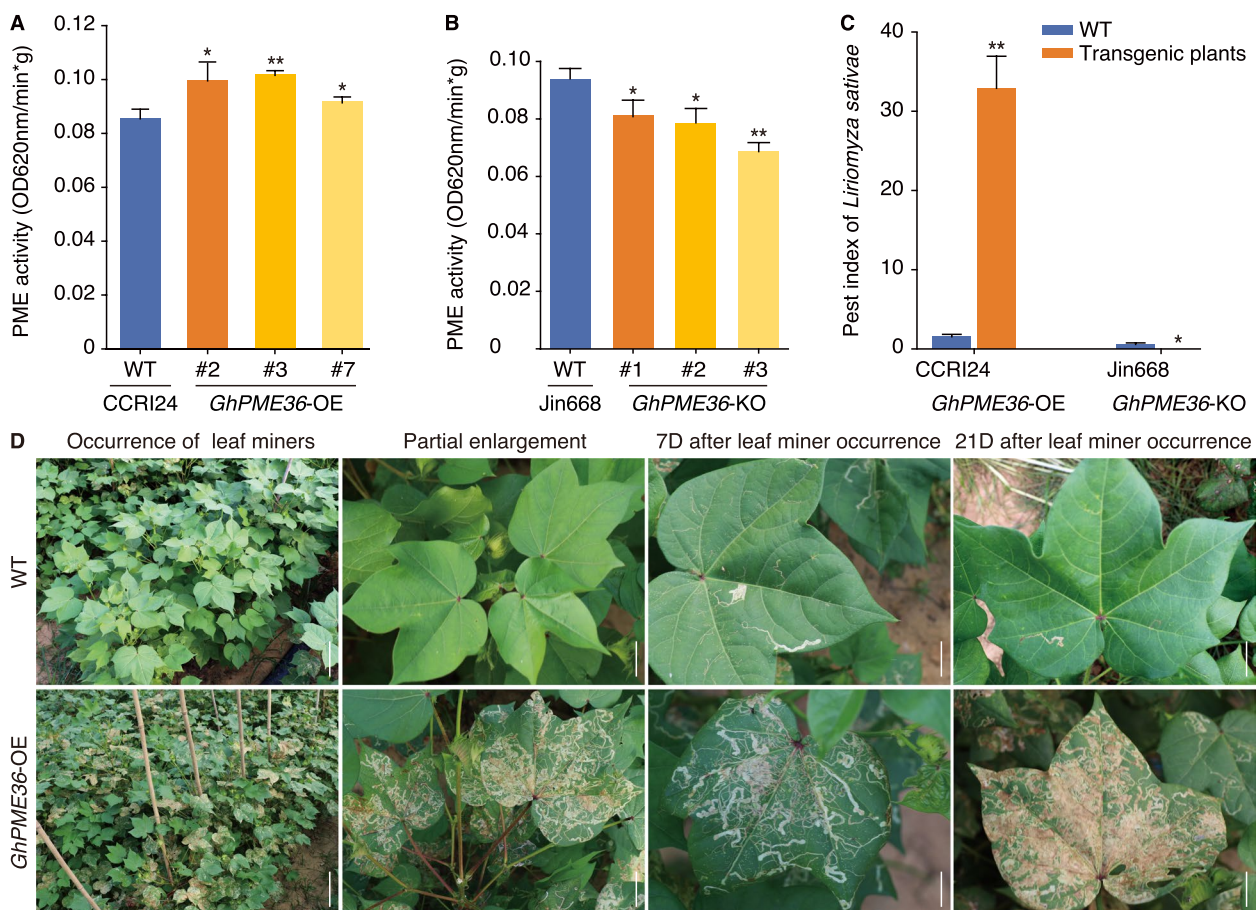


**Fig. 3** PME activity and leaf miner susceptibility of *GhPME36*-OE and *GhPME36*-KO cotton. **A** PME activity in three *GhPME36*-OE cotton lines, with CCRI24 as the WT. **B** PME activity in three *GhPME36*-KO cotton lines, with Jin668 as the WT. **C** Pest indices of the *GhPME36*-OE and *GhPME36*-KO lines. The data are presented as the means  $\pm$  SDs ( $n = 3$  biological replicates). Asterisks indicate significant differences compared with WT (\* $P < 0.05$ , \*\* $P < 0.01$ ;  $t$ -test). **D** Leaf miner damage of WT and *GhPME36*-OE cotton leaves in the field. Scale bar, 6 cm

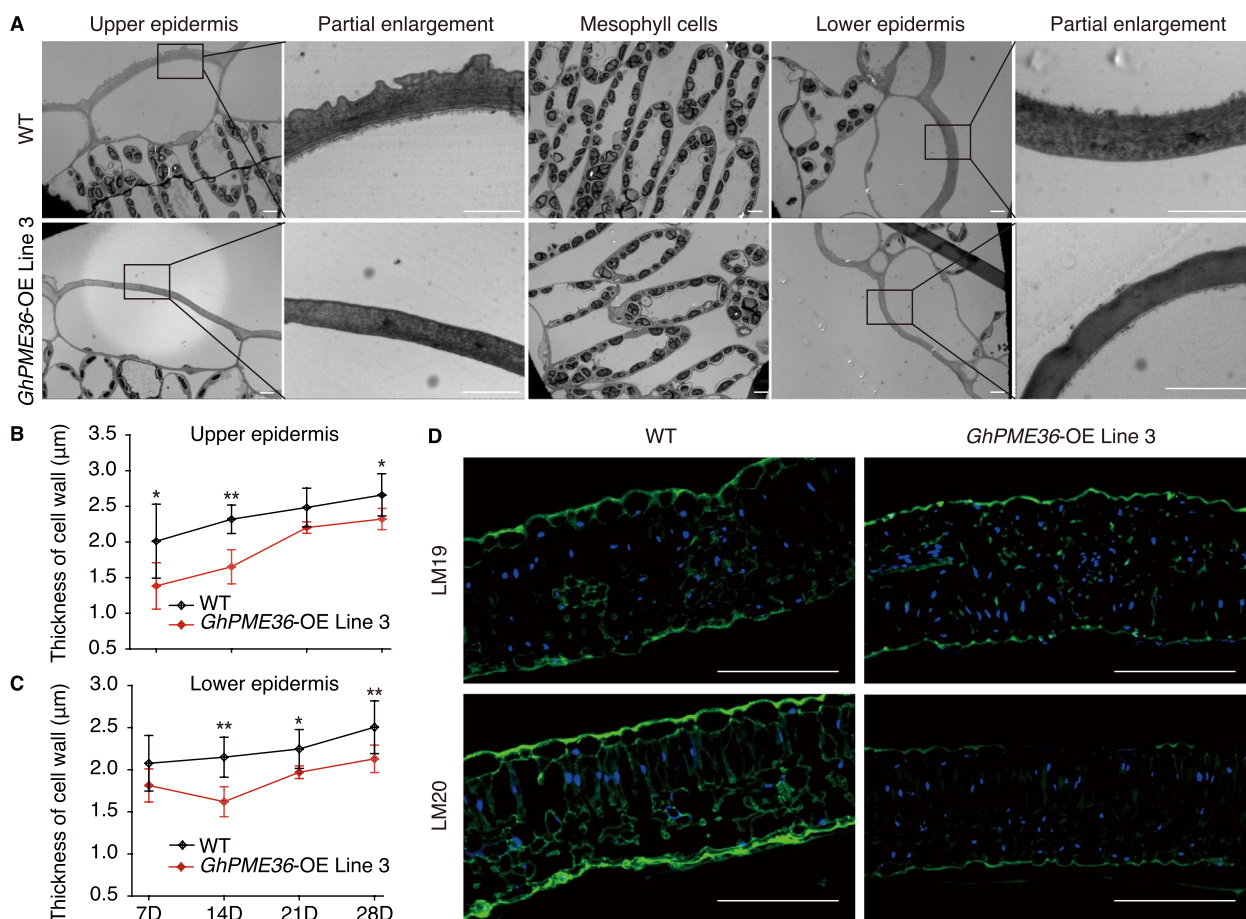


**Fig. 4** Pectin methylesterification and morphology of epidermal cells in *GhPME36*-OE line 3 cotton leaves. **A** TEM observation of longitudinal sections of WT and *GhPME36*-OE cotton leaves. Scale bar, 5 nm. **B, C** Thickness of the cell walls of the upper (**B**) and lower (**C**) epidermis of WT and *GhPME36*-OE cotton leaves. The data are presented as the means  $\pm$  SDs ( $n=5$  biological replicates). Asterisks indicate significant differences compared with WT (\* $P < 0.05$ , \*\* $P < 0.01$ ;  $t$ -test). **D** Pectin methylesterification of the leaf epidermis indicated by LM19 and LM20 antibodies in WT and *GhPME36*-OE cotton leaves. Scale bar, 200  $\mu$ m

Considering that *GhPME36* encodes a pectin methyl-esterase, the construction of leaf cell pectin might be responsible for the increased susceptibility of the *GhPME36*-OE cotton plants to leaf miners. Pectin methylesterification was then determined by immunofluorescence using two monoclonal antibodies, namely, LM19 and LM20, which label low-level methylesterified pectin and highly methylesterified pectin, respectively. In the epidermal cells of *GhPME36*-OE cotton leaves, the amount of highly methylesterified pectin was significantly lower than that in the WT plants. However, there were few differences between them in the amount of pectin methylesterified at a low level (Fig. 4D). Analysis of mesophyll cell morphology distinctly revealed that the palisade tissue of the *GhPME36*-OE cotton leaves was looser than that of the WT leaves (Fig. 4A), which made it more conducive to leaf miner feeding.

The transcriptomes of cotton leaves from the *GhPME36*-OE and WT plants were sequenced to explore the underlying mechanism further. The quality control of the sequencing data is shown in Additional file 2: Table S2. In total, 1948 differentially expressed genes (DEGs) were identified, of which 798 DEGs were upregulated and 1150 DEGs were downregulated (Additional file 1: Fig. S5). Among them, multiple genes encoding enzymes associated with cell wall polysaccharide synthesis were identified. For example, six polygalacturonase (PG) genes were upregulated 2- to fourfold, one pectinesterase (PE) gene was upregulated 2.5-fold, and two xylanase (Xyl) genes were upregulated 3.5- and fivefold. Moreover, the expression levels of two PE genes, two  $\beta$ -galactosidase ( $\beta$ -Gal) genes, and five Xyl genes were reduced by at least 53% (Additional file 2: Table S3). These genes have been reported to depolymerize and secrete cell wall polysaccharides to the plant surface

in the form of gum during MeJA-induced gummosis in peach [51]. Thus, it was speculated that the alteration of these genes also facilitated the conversion of cell wall polysaccharides to a form more accessible to leaf miners.

#### Glucose synthesis was affected in *GhPME36*-OE cotton leaves

To further explore the cell wall components of the *GhPME36*-OE cotton leaves, the CWM was extracted and evaluated. Compared with that of the WT, the cell wall material (CWM) content was significantly (5–10%) lower in the three *GhPME36*-OE lines (Additional file 1: Fig. S6A) but 6–13% higher in the three *GhPME36*-KO lines (Additional file 1: Fig. S6B).

Previous studies have reported that changes in sugar content can effectively affect the feeding behavior of insects [52, 53]. To explore the influence of the sugar content of cotton leaves on their susceptibility to leaf miners, the soluble sugar content was measured during seven developmental stages. The results revealed that the most significant difference between the *GhPME36*-OE and WT plants occurred in the middle and late stages of leaf development (Additional file 1: Fig. S7). During the late developmental stage, the soluble sugar content in the leaves of the three *GhPME36*-OE cotton lines was 20–30% higher than that of the WT (Fig. 5A), and that of the three *GhPME36*-KO cotton lines was 12–20% lower (Fig. 5B).

Targeted metabolome analysis was conducted to explore the key metabolites among the 13 monosaccharides/disaccharides in the *GhPME36*-OE cotton leaves. The results revealed higher contents of most commonly detected sugars, especially D-fructose (94%) and glucose (96%) (Additional file 1: Fig. S8). The KEGG annotation and enrichment analyses revealed that the identified metabolites were enriched mainly in glycolysis/gluconeogenesis, the pentose phosphate pathway, and starch and sucrose metabolism (Additional file 1: Fig. S9). The DEGs identified via transcriptome sequencing were enriched mainly in the biosynthesis of secondary metabolites, metabolic pathways, and starch and sucrose metabolism (Additional file 1: Fig. S9). Moreover, conjoint metabolome and transcriptome analysis revealed that 1761 DEGs were related to the identified metabolites. Among them, 715 DEGs were upregulated, and 1046 were downregulated (Fig. 5C). Glucose was determined to be the key differentially accumulated metabolite, given that multiple glucose-related metabolic pathways and 242 DEGs were affected (Fig. 5D).

The KEGG pathway Ko00010 was selected for further research because of its low P value (Additional file 2: Table S4) and its important role in glucose metabolism. Nine of the 13 DEGs enriched in the Ko00010 pathway

were selected for further analysis according to their FPKM (fragments per kilobase of transcript per million fragments mapped) values (Additional file 2: Table S5). The FPKM values of four genes was 2- to 3.5-fold higher and those of the other five genes were at least 53% lower than those of the WT (Additional file 2: Table S5). The relative expression levels of these genes were verified via qPCR, and the results were essentially consistent with the transcriptome data (Fig. 5E). Among them, *GH\_A10G1251* and *GH\_A06G0364*, annotated as pyruvate kinase and alcohol dehydrogenase, respectively, are regarded as two key genes because of their severe down regulation of expression. The significant reduction in their expression levels might have decreased the metabolic rate of phosphorylated pyruvate and acetaldehyde, thereby leading to an excessive accumulation of D-glucose. The results above indicated that the expression of numerous genes was differentially influenced in the leaves of the *GhPME36*-OE cotton plants, and 242 of these DEGs further affected glucose metabolism through multiple pathways, such as glycolysis and gluconeogenesis, ultimately leading to a significant increase in glucose content. The increase in glucose content might increase the attraction of leaf miners to the leaves and ultimately increase the susceptibility of *GhPME36*-OE cotton to leaf miners.

#### Responses of *GhPME36*-OE to leaf miner attack

When plants are subjected to damage caused by insects, a biotic stress response occurs that includes the initiation of defense signaling pathways and the activation of the expression of related genes. According to the KEGG enrichment of DEGs, 38 DEGs were enriched in the flavonoid and phenylpropanoid biosynthesis pathways. Flavonoid biosynthesis is associated with oxidative stress and mechanical damage [54, 55], whereas phenylpropanoid metabolic biosynthesis plays a coordinated role in plant–environment interactions [56]. A total of 27 out of 38 DEGs were upregulated 2- to sixfold (Additional file 2: Table S6). The relative expression levels of the 12 most abundant DEGs encoding ascorbate-dependent oxidoreductase (ANS), bifunctional dihydroflavonol 4-reductase flavanone (DFR), peroxidase (POD), anthocyanidin reductase (ANR), and 4-coumarate-CoA ligase (4CL3) were determined and found to be consistent with the transcriptome data (Additional file 1: Fig. S10–S11).

The jasmonic acid (JA) signal transduction pathway also plays a role in plant defense signal transduction [57]. Among the 798 upregulated DEGs, two encoding lipoxygenase (LOX) and five encoding jasmonate ZIM-domain (JAZ) proteins were upregulated 2–fivefold in *GhPME36*-OE cotton leaves (Additional file 2: Table S7). The relative expression levels of the four candidate DEGs were

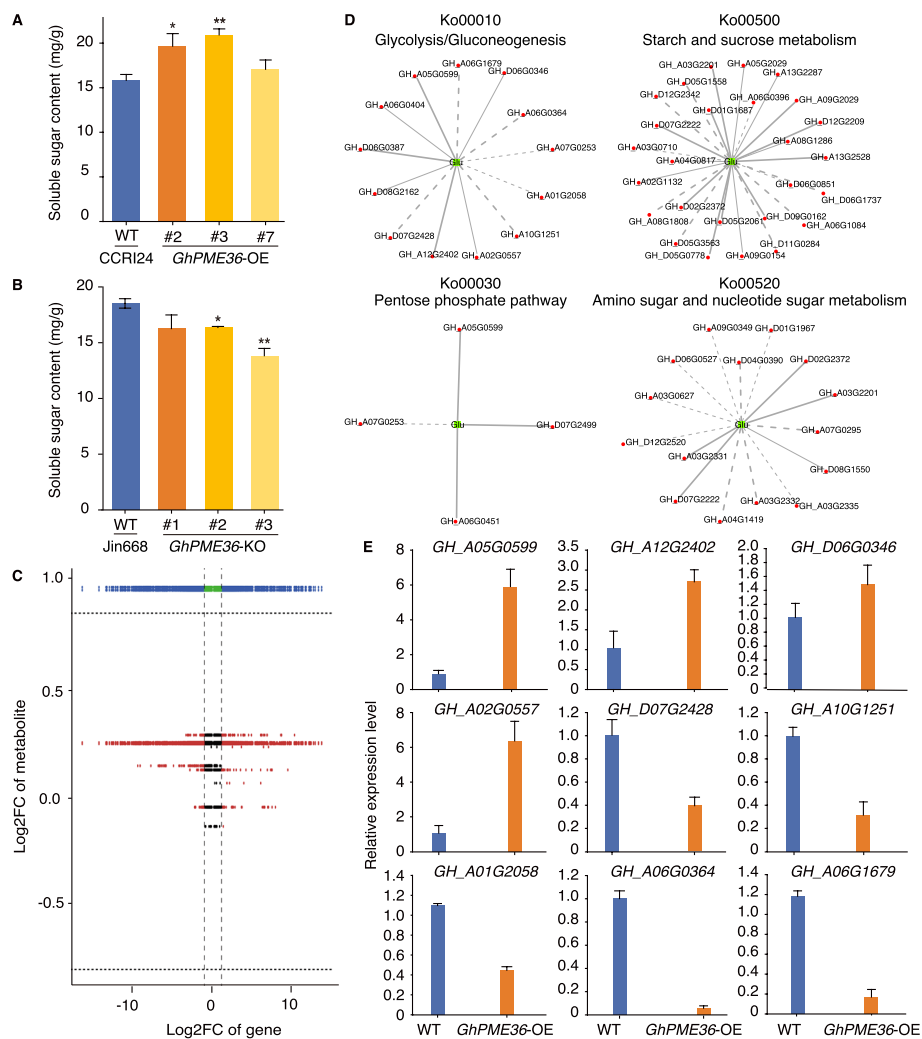


**Fig. 5** Differentially accumulated metabolites and DEGs between WT and *GhPME36*-OE cotton leaves. **A, B** Soluble sugar content of cotton leaves from three *GhPME36*-OE lines (**A**) and three *GhPME36*-KO lines (**B**). The data are presented as the means  $\pm$  SDs ( $n = 5$  biological replicates). Asterisks indicate significant differences compared with WT (\* $P < 0.05$ , \*\* $P < 0.01$ ;  $t$ -test). **C** Conjoint analysis of metabolites and genes in nine quadrants. Quadrant 1: The tendencies of genes and metabolites are opposite. Quadrant 3: The tendencies of genes and metabolites are consistent. **D** Correlation network of metabolites and genes. Metabolites are represented by green dots, while genes are represented by red dots. The solid lines indicate positive correlations, whereas the dotted lines indicate negative correlations. PCCs  $> 0.80$ ,  $P$  value  $< 0.05$ . **E** qPCR analysis of DEGs involved in the Ko00010 pathway

consistent with their FPKM values (Additional file 1: Fig. S12).

### GhC/VIF1 interacted with GhPME36

As stated previously, the regulatory interaction between PME1 and PME has been reported in a few plant species. To explore whether GhPME36 functions through interactions with some PMEIs in cotton leaves, all potential PMEIs in cotton leaves were screened, and their evolutionary relationships are displayed in a phylogenetic tree (Additional file 1: Fig. S13). All the *GhPMEIs* were ranked in descending order according to their

expression levels in the leaves, among which five *PMEI* genes were noted because of their high expression (Additional file 2: Table S8). Considering that both *GhPME36* (*GH\_D11G0862*) and *GhC/VIF1* (*GH\_D10G1994*) were located in D genome, *GhC/VIF1* was further selected as the candidate gene.

The PRO region of type I PMEs, including the PME1 domain, is often considered to inhibit the maturation of PME domains [58, 59]. To avoid this inhibition, GhPME36 without a signal peptide (GhPME36-X1) and without a PRO region (GhPME36-X2) were separately amplified (Fig. 6A). Y2H assays demonstrated that

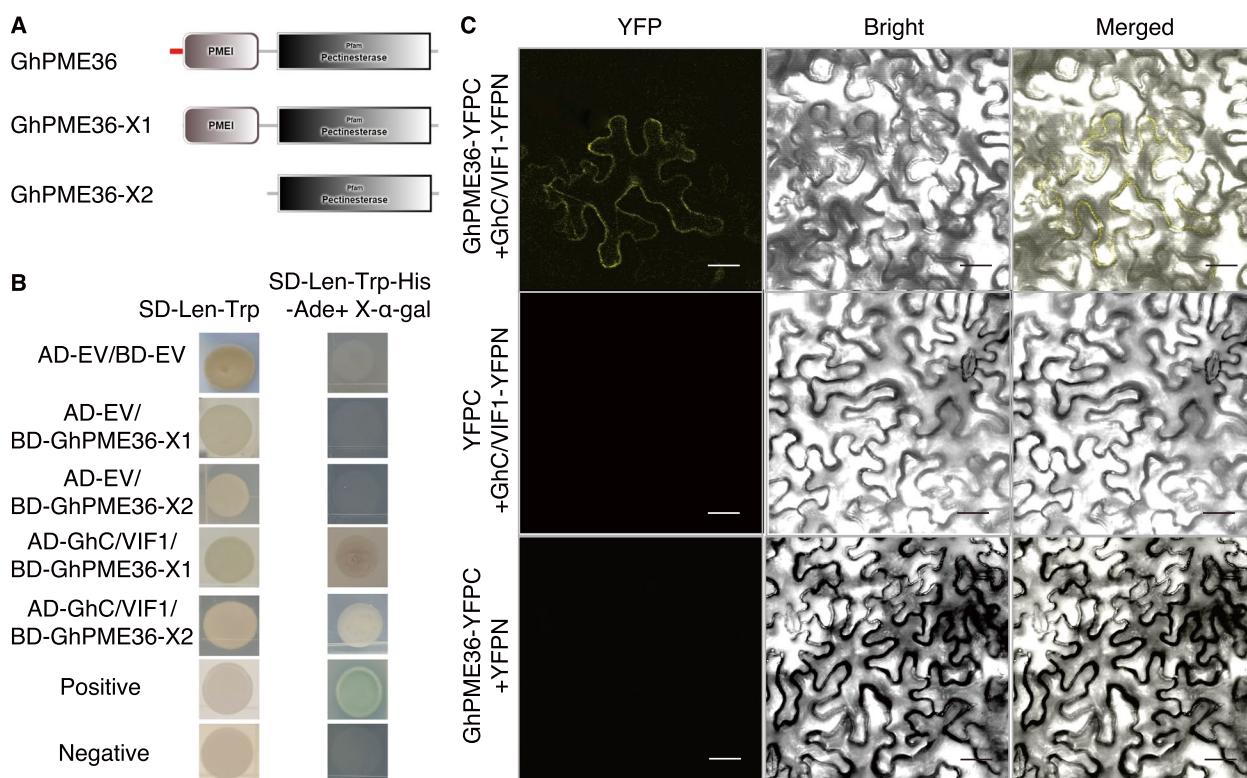


**Fig. 6** Protein interaction between GhPME36 and GhC/VIF1. **A** Vector construction for the Y2H assay. GhPME36-X1 lacked the signal peptide, whereas GhPME36-X2 lacked the signal peptide and the PME domain. **B**, **C** Y2H (**B**) and BiFC (**C**) assays for GhPME36 and GhC/VIF1. Scale bar, 40 μm

different fragments of the GhPME36 protein could interact with GhC/VIF1 (Fig. 6B). BiFC was carried out for further validation, which revealed that GhPME36 interacted with GhC/VIF1 in the cell wall (Fig. 6C), which was consistent with the subcellular localization of GhPME36. These results suggested that GhPME36 interacted with GhC/VIF1 through the combination of the PME and PME domains and that the presence of the PRO region did not affect the interaction between GhPME36 and GhC/VIF1.

### Discussion

PMEs in higher plants are encoded by a polygene family. It has been reported that members of the PME family play a role in various plant tissues and organs, such as the seed coat [36], pollen tube [37], stem [38], and fruit [34]. In this study, a member of the cotton PME family, namely, GhPME36, was identified. According to published transcriptome data [60], *GhPME36* is widely expressed in multiple organs/tissues, including roots, stems, leaves and flowers (Additional file 1: Fig. S1A). During fiber development, the high expression of *GhPME36* decreased during the late stage (Additional file 1: Fig. S1B), with a significant change in the morphology of the cell wall [61]. The expression patterns of *GhPME36* during different

leaf developmental stages were analyzed via qPCR. Its expression level decreased during early developmental stages but increased during the late developmental stages (Fig. 1A). In addition, a GUS staining assay revealed that the promoter of *GhPME36* was active in root hairs, young stems, leaf veins, calyxes, and both pod ends in *Arabidopsis* (Fig. 1C). The expression pattern of *GhPME36* was consistent with that of other reported PME genes, which are widely expressed during most developmental stages of various organs and tissues.

PME family proteins can be classified as type I and type II. GhPME36 contains both PME and PME domains (Fig. 6A) and thus belongs to the type I category. Most reported type I PMEs are located in the cell wall [35, 62]. This study revealed through subcellular localization experiments in tobacco leaves (Additional file 1: Fig. S2) and onion epidermal cells (Fig. 1B) that GhPME36 was also located in the cell wall.

A previous study reported that the interaction between PMEs and PMEIs was strongly affected by pH, and their dissociation constant in acidic solution was 10 times lower than that in neutral solution [44]. Moreover, the process of pectin demethylesterification can affect the environmental pH [63]. Thus, there are several obstacles to directly verifying interactions between PMEs and

PMEIs. Researchers have demonstrated their interaction by determining the inhibition efficiency of PMEIs on PMEs [64]. In this study, the interaction between GhPME36 and GhC/VIF1, a PMEI, was verified through Y2H and BiFC assays (Fig. 6B, C). However, whether GhC/VIF1 has inhibitory efficiency on the enzymatic activity of GhPME36 requires chemical evidence to confirm. The PMEI gene family has been explored in a variety of plants and has been found to have approximately the same number of members as the PME gene family [65]. However, the corresponding relationships between PMEs and PMEIs are not "monogamous" as might be expected. Some PMEIs have extensive inhibitory effects on multiple PMEs, even PMEs from different species [66, 67]. Whether GhPME36 has other interacting proteins and whether GhPME36 interacts with other PMEIs require further exploration.

It has been reported that the N-terminal PRO region is an inhibitor of PME activity [58, 59], which prevents premature demethylesterification of pectins before their secretion by binding the PME domain [43]. Though the changes of *GhPME36* expression affected PME activity (Fig. 3A, Additional file 1: Fig. S3B), whether GhPME36 had PME enzyme activity would be confirmed by heterologously expressing it in *Pichia pastoris* or *E. coli* without its pro region. In this study, Y2H experiments demonstrated that GhPME36 can interact with GhC/VIF1, albeit weakly, regardless of the presence of a PRO region (Fig. 6A, B).

Cell wall softening and hardening are determined by two subsequent fates of demethylated pectin, i.e., crosslinking with divalent cations and degradation [68]. High methylesterification of pectin in *Arabidopsis* stems causes a reduction in cell wall thickness and overall mechanical strength [38]. Pectin demethylesterification in pollen tubes increases cell wall hardness [69], but several studies have shown that increased PME activity plays a positive role in fruit softening [34].

The content of highly methylesterified pectin decreased significantly, whereas that of pectin methylesterified at low levels did not change substantially in the *GhPME36*-OE cotton leaves (Fig. 4A). The pectin of *Arabidopsis* with heterologous expression of *PME* was found to be more easily degraded by polygalacturonase [41]. We speculated that unplanned demethylesterification initiated pectin degradation, and thus, no additional pectin methylesterified at low levels was detected. Demethylesterification is the first step in the degradation of pectin, and PMEs may act as the "first cause" in the process of pectin degradation. In this study, pectin demethylesterification in the epidermis of leaves by GhPME36 led to softening rather than hardening of the cell wall, in contrast to the findings of previous studies. Thus, pectin

demethylesterification has two different effects on the cell wall: hardening during elongation development and softening during expansion development.

PME is related to biotic and abiotic stresses, such as that caused by aphids [15], fungi [64], bacteria [70], nematodes [71, 72], salt [40], and drought [35]. In this study, *GhPME36*-OE cotton was highly susceptible to leaf miners (Fig. 3C, D), which revealed the relationship between PME and leaf miner resistance in cotton for the first time. To explore the material foundation and molecular mechanism behind this phenomenon, we carried out a series of experiments. The contents of most sugars in the leaves, with the exception of pectin, was higher in the *GhPME36*-OE cotton leaves (Additional file 1: Fig. S7). Transcriptome analysis revealed that most DEGs affected by *GhPME36* were annotated in the biosynthesis of secondary metabolites, metabolic pathways, and starch and sucrose metabolic pathways. These findings are consistent with the metabolome results (Additional file 1: Fig. S8). The Ko00010 metabolic pathway and nine key DEGs in this pathway (Additional file 2: Table S5) were screened based on the *P* value of the differentially accumulated metabolites. The results of the qPCR verification of these nine genes were consistent with the transcriptome data (Fig. 5E). It has been reported that plant water-soluble substances affect host selection in *Liriomyza sativae* [73]. Additionally, the stage with obvious differences in sugar content coincided with the leaf miner breakout stage (Fig. 3D, Additional file 1: Fig. S6).

It has been reported that mutations that affect cell wall biosynthesis can cause knock-on effects on carbohydrate metabolism [26]. Taken together, our results revealed that the overexpression of *GhPME36* reduced the content of highly methylesterified pectin in cotton leaves (Fig. 4A) and hindered the thickening of cell walls (Fig. 4B–D). These defects may influence multiple pathways, such as starch and sucrose metabolism, glycolysis/gluconeogenesis, and the pentose phosphate pathway, to increase the glucose content (Fig. 5D), ultimately affecting the host selection of *Liriomyza sativae*. The mechanism by which *GhPME36* aggravates the susceptibility of cotton leaves to *Liriomyza sativae* is shown in Fig. 7. The plant–insect interaction revealed by these findings may also be applicable to phytophagous insects such as aphids and ants, which are sensitive to sugar.

## Conclusions

In conclusion, by observing the cell wall structure and identifying DEGs and differentially accumulated metabolites in *GhPME36*-OE cotton leaves, this study comprehensively elucidates the cytological and molecular mechanisms by which GhPME36 exacerbates the susceptibility of cotton leaves to *Liriomyza sativae*. A new

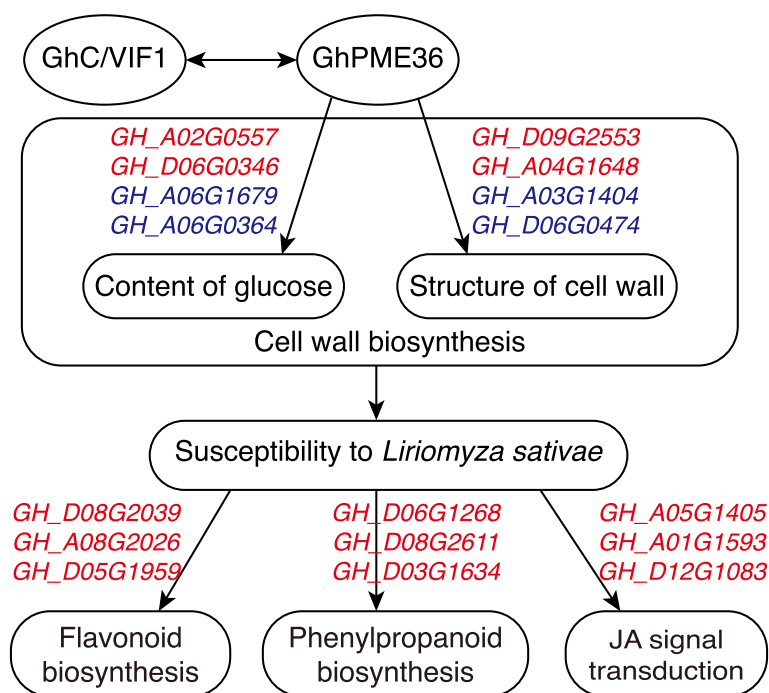


**Fig. 7** Mechanism by which *GhPME36* aggravates the susceptibility of cotton leaves to *Liriomyza sativae*. The upregulated genes are represented in red, whereas the downregulated genes are represented in blue

strategy for *Liriomyza sativae* resistance is proposed to reallocate glucose inside crop leaves. These findings shed considerable light on PME function and provide an environmentally friendly approach for crop genetic improvement.

## Methods

### Plant materials and growth conditions

The upland cotton cultivars CCRI24 and Jin668 were obtained from the Institute of Cotton Research of the Chinese Academy of Agricultural Sciences (CAAS) and were used as WT. Tobacco (*Nicotiana benthamiana*) and Arabidopsis Col-0 plants were preserved in our laboratory.

Cotton seeds were sown in the experimental plots on April 23, 2021, and April 20, 2022 (Zhengzhou, China), in a greenhouse at  $28 \pm 2$  °C under an external natural light intensity of 40–60%. Arabidopsis and tobacco were grown in a culture room under continuous light ( $70$  to  $80 \mu\text{mol m}^{-2} \text{s}^{-1}$ ) at  $28 \pm 2$  °C and  $23 \pm 2$  °C, respectively. All the plants were grown on a mixture of nutritive soil and vermiculite (2:1).

### qPCR analysis

Expression data for *GhPME36* in various cotton organs and tissues was retrieved from *Gossypium hirsutum* cultivar TM-1 transcriptome data [60]. Total RNA was

isolated from *GhPME36*-OE and WT cotton leaves at 7, 14, 21, 28, and 35 days after leaf spreading (D) with TRIzol-A<sup>+</sup> Reagent (TaKaRa, Japan) and used to synthesize cDNA with Recombinant NovoScript Plus All-in-one 1st Strand cDNA Synthesis SuperMix (Novoprotein, China). The qPCR experiment was performed with PerfectStart Green qPCR Super Mix (TransGen, China) in an optical 384-well plate using an ABI PRISM 7500 real-time PCR system (Applied Biosystems). A 20- $\mu\text{L}$  reaction consisted of 1  $\mu\text{g}$  of cDNA, 0.2  $\mu\text{M}$  forward and reverse primers, and 10  $\mu\text{L}$  of TransStart Green qRT-PCR Super Mix. Relative expression data were calculated via the Livak method ( $2^{-\Delta\Delta\text{Ct}}$ ) [74]. Each result was composed of three biological and three technical replicates. Primers used for qPCR were listed in Additional file 2: Table S9.

### Vector construction and plant transformation

The *GhPME36* coding sequence (CDS, 1.56 kb) was amplified using KOD One™ PCR Master Mix (Toyobo, Japan). The amplicon was subsequently cloned and inserted into a pBI121 Plant Expression Vector (Solarbio, China) under the control of the 35S promoter with a ClonExpress Ultra One Step Cloning Kit (Vazyme, China). Two CRISPR target sites (ATGATGTGAGATCATGGTGC; GTGCGGCACGCTCTAGAGCG) were designed according to the mRNA and corresponding genomic DNA sequence information of *GhPME36* as

well as its homologs. The fragment containing the target sites was amplified and then cloned and inserted into the CRISPR expression vector pCAS9/gRNA3 via the ClonExpress Ultra One Step Cloning Kit.

Constructed vectors 35S:*GhPME36*:pBI121 and pCAS9/gRNA3 were transformed into cotton plants via *Agrobacterium*-mediated transformation [75]. Primers used for transgenic cotton identification were listed in Additional file 2: Table S9. Transgenic Arabidopsis was obtained via infection of Arabidopsis Col-0 via the floral dip method [76], followed by screening on MS agar media supplemented with 50 mg/L kanamycin.

#### GUS staining

The 1500-bp sequence upstream of *GhPME36* was amplified from upland cotton genomic DNA to construct a pro*GhPME36*:*GUS* expression vector, which was transformed into *Agrobacterium tumefaciens* GV3101 and subsequently used to infect Arabidopsis Col-0 via the floral dip method [76]. Harvested seeds were screened with MS agar media supplemented with 50 mg/L kanamycin until homozygous lines were obtained. Roots, stems, leaves, flowers, and pods were cultured in GUS staining solution containing 1 mM 5-bromo-4-chloro-3-indolyl-glucuronide for 24 h at 37 °C and then decolorized in 70% ethanol for 24–48 h. Images were recorded via a research-grade photographic stereomicroscope (Leica M165C).

#### Subcellular localization

The pCAMBIA2300-35S-*GhPME36*-eGFP vector was constructed using the *GhPME36* CDS and transferred into tobacco leaves and onion inner epidermis via *Agrobacterium tumefaciens* GV3101. After 2 days of culture (25 °C, 24 h dark/24 h light), tobacco leaves were treated with 0.4 g/ml sucrose solution for plasmolysis. GFP images were then obtained with a laser scanning confocal microscope (OLYMPUS FV1200).

The onion inner epidermis was spread on MS agar media supplemented with 100 mg/l ampicillin and pre-cultured for 4 h (in the dark at 25 °C). A total of 3 mg of gold powder (Bio-Rad, America) in a 1.5-mL centrifuge tube was sterilized with 75% alcohol for 15 min, washed with ddH<sub>2</sub>O three times, and resuspended in 50 µL of 50% glycerin. A mixture containing 5 µL of plasmid (1 µg/µL), 50 µL of CaCl<sub>2</sub> (2.5 M/L), and 20 µL of spermidine (0.1 M/L) was added to the tubes, which were mixed for 2–3 s after each addition, and the suspension–precipitation method was conducted 10 times to enhance the binding between the plasmid and gold powder. The gold powder with the plasmid was washed, resuspended in ethanol, and then injected into the onion inner epidermis by Gene Gun (PDS-1000). The instrument

parameters were as follows: split film, 1350 psi; vacuum degree, 26–28 in Hg; and bombardment distance, 6 cm. After being cultured for 24–48 h (25 °C in the dark), GFP images were obtained with a laser scanning confocal microscope (OLYMPUS FV1200) before and after the onion inner epidermis was treated with 0.3 g/ml sucrose solution for plasmolysis.

#### PME activity assay

PME activity was determined via Hagerman's method [77] and adjusted accordingly in 40-day-old cotton leaves. One gram of ground fresh cotton leaves was placed into 5 ml of 8.8% NaCl (4 °C), mixed and centrifuged (8000 rpm) for 10 min to collect the supernatant, and the pH was adjusted to 7.5. The reaction system contained 4 ml of 0.5% pectin solution, 0.3 ml of 0.01% bromophenol blue, and 0.3 ml of supernatant. The absorbance value was measured after 2 min. The enzyme activity was represented as  $\Delta A_{620}/\text{min}\cdot\text{g}$ .

#### Pest index statistics

The level of leaf miner damage was examined via a five-point sampling method. The pest index was determined according to the methods of Luo et al. [78], with slight modifications. Three-month-old cotton plants grown in the field were used for investigation. Ten plants were used at each point, and three leaves per plant were sampled. Pest index =  $100 \times \Sigma (\text{number of affected leaves} \times \text{victim grade}) / (\text{total number of leaves examined} \times \text{highest grade of victimization})$ .

#### Transmission electron microscopy observation

Slices (5 mm × 20 mm) from the middle right side of the leaf vein were collected from cotton leaves at different stages (7, 14, 21 and 28 D) and fixed with a 2.5% glutaraldehyde solution in 0.2 M PBS buffer (pH 7.4) for 1 h under vacuum and for 24 h at room temperature. The sections were washed in 0.2 M PBS buffer (pH 7.4) three times and postfixed with 1% osmium tetroxide for 1 h. After being washed in 0.2 M PBS buffer (pH 7.4) three times, the sections were dehydrated in a gradient of 50–100% acetone and embedded in EPON 812 resin. Ultrathin sections were cut with an ultramicrotome, collected on Formvar-coated copper grids, and stained with 2% uranyl acetate. The samples were observed with an HT7800 transmission electron microscope (HITACHI) at 80 kV and measured with Image-Pro Plus 6.0.

#### Determination of soluble sugar content

Forty-day-old cotton leaves were used for determination of CWM. The extraction of cotton leaf cell walls was performed according to Jia et al. [18]. The soluble sugar content was determined via a plant soluble sugar assay kit

(Solarbio). A total of 0.1 g of leaves at different stages (7, 14, 21, 28, and 35 D) from the transgenic cotton and WT plants were harvested. After being ground in liquid nitrogen, the samples were boiled in a water bath for 10 min with 1 mL of ddH<sub>2</sub>O and centrifuged at 8000 rpm for 10 min at room temperature after cooling to collect the supernatant as the sample mixture. The experimental system contained 40  $\mu$ L of sample mixture, 40  $\mu$ L of ddH<sub>2</sub>O, 20  $\mu$ L of 2% anthrone (dissolved in ethyl acetate) and 200  $\mu$ L of concentrated sulfuric acid. After 10 min in a 95 °C water bath, the absorbance value at 620 nm was measured after cooling. A standard curve was established, and  $\Delta A_{620}$  was converted to the soluble sugar content. Each sample was conducted in triplicate.

### Immunofluorescence localization

Slices (10 mm  $\times$  40 mm) from the middle right side of the leaf vein were collected from mature cotton leaves and fixed with a 4% paraformaldehyde solution in 0.2 M PBS buffer (pH 7.4) for 12–24 h at room temperature. The methods of embedding, sectioning, and immunofluorescence labeling for the samples were previously described by Vitha and Osteryoung [79]. The antibodies LM19 and LM20 (Kerafast, United States) used in this study were diluted 1:50. Images were acquired with a digital slide scanner (Leica SCN400) and analyzed with the Aperio ImageScope software.

### Omics analysis

Mature cotton leaves were collected from the *GhPME36*-OE and WT plants and stored at –80 °C after they were frozen in liquid nitrogen.

The samples used for transcriptome analysis were ground and used to isolate total RNA. The purity of the RNA was determined via Nanodrop and agarose gel electrophoresis. The constructed library was sequenced on an Illumina HiSeq™ 2000 platform (Berry Genomics, China). The raw reads were filtered via quality control (QC). Clean reads were aligned to the upland cotton reference genome (<http://cotton.zju.edu.cn/>) via HISAT2 (<https://daehwankimlab.github.io/hisat2/>). Read counts were recorded with StringTie [80]. The DEGs were identified with the DESeq2 R package [81]. KEGG annotation and enrichment were achieved using Kobas (kobas.cbi.pku.edu.cn) and kofamKOALA (<https://www.genome.jp/tools/kofamkoala/>).

Samples for targeted metabolome analysis were ground (30 Hz, 1.5 min) to powder after vacuum freeze-drying. A total of 20 mg of powder was added to 500  $\mu$ L of extraction solution (methanol: isopropanol: water = 3:3:2, V/V/V). The mixture was swirled for 3 min and ultrasonicated in ice water for 30 min. Fifty microliters of the supernatant was removed after centrifugation (4 °C,

14,000 r/min) for 3 min, 20  $\mu$ L of internal standard solution (1000  $\mu$ g/mL) was added, and the mixture was concentrated with nitrogen and freeze-dried. Then, 100  $\mu$ L of ammonium methoxide pyridine (15 mg/mL) was added to the solution and incubated at 37 °C for 2 h. Then, 100  $\mu$ L of BSTFA was added to the solution and incubated at 37 °C for 30 min to obtain the derivatization solution. The solution was diluted to 1 mL with n-hexane for GC–MS (8890-5977B, Agilent) analysis, and the scanning mode used was selective ion monitoring mode. The content of the substance in the sample was calculated by substituting the integration of the peak areas into the standard curve linear equation.

### Protein–protein interactions

To screen potential interacting PMEIs, *Gossypium hirsutum* protein data [60] were downloaded from the State Key Laboratory of Crop Genetics and Germplasm Enhancement (<https://mascotton.njau.edu.cn/info/1054/1118.htm>). A hidden Markov model of the conserved PME domain (PF04043) was obtained from the Pfam database (<http://pfam.xfam.org/>). An HMM search in HMMER 3.0 software was used to analyze protein sequences (the e value was set to be less than  $1 \times 10^{-10}$ ). A total of 260 possible *PMEI* genes were predicted. Batch CD-Search (<https://www.ncbi.nlm.nih.gov/Structure/bwrpsb/bwrpsb.cgi>) was subsequently used to analyze the *PMEI* domains, and sequences containing incomplete domains were deleted. Smart online analysis software (<http://smart.embl-heidelberg.de/>) was used to analyze candidate sequences. Protein sequences containing both PME and *PMEI* domains (type I PMEs) were deleted. Finally, 130 *PMEI* family proteins were identified.

For yeast two-hybrid assay (Y2H), the protein domains of *GhPME36* analyzed via SMART online tools (<https://smart.embl.de/>), and pGBKT7-*GhPME36* and pGADT7-*GhC/VIF1* were constructed and cotransformed into the Y2H Gold Yeast strain (Weidi, China). Transformed colonies were first grown on SD/-Leu/-Trp agar media for 2 days and then transferred into SD/-Ade/-His/-Leu/-Trp agar media supplemented with X- $\alpha$ -Gal. After growing for 2 days at 30 °C in the dark, colonies that grew and appeared blue were considered positive.

For bimolecular fluorescence complementation (BiFC), the CDS of *GhPME36* was fused to the C-terminus of the pXY104-cYFP vector, while *GhC/VIF1* was fused to the N-terminus of the pXY106-nYFP vector. pXY104-*GhPME36*-cYFP and pXY106-*GhC/VIF1*-nYFP were separately transformed into *Agrobacterium tumefaciens* GV3101 (Weidi, China) and expressed in tobacco leaves (25 °C, 4 weeks) via coinjection. After 2 days (25 °C, 24 h dark/24 h light), YFP images were obtained with a laser

scanning confocal microscope (OLYMPUS FV1200) with an ultraviolet spectrum excitation of 488 nm.

### Statistical analysis

Two-tailed unpaired Student's *t*-test was performed for comparing two groups of data. Duncan's multiple range tests were used for multiple groups of data. The confidence coefficient was set at  $0.01 < *P < 0.05$ ,  $**P < 0.01$ .

### Abbreviations

PME	Pectin methylesterase
HG	Homogalacturonan
PMEI	Pectin methylesterase inhibitor
MeOH	Methanol
DEG	Differentially expressed gene
PG	Polygalacturonase
PE	Pectinesterase
Xyl	Xylanase
$\beta$ -Gal	$\beta$ -galactosidase
FPKM	Fragments per kilobase of transcript per million fragments mapped
ANS	Ascorbate-dependent oxidoreductase
DFR	Dihydroflavonol 4-reductase flavanone
POD	Peroxidase
ANR	Anthocyanidin reductase
4CL3	4-coumarate-CoA ligase
JA	Jasmonic acid
LOX	Lipoxygenase
JAZ	Jasmonate ZIM-domain
CWM	Cell wall material

### Supplementary Information

The online version contains supplementary material available at <https://doi.org/10.1186/s12915-024-01999-7>.

Additional file 1. Fig. S1. Expression of GhPME36 in various cotton organs and tissues. Fig. S2. Subcellular localization of GhPME36 in tobacco leaves. Fig. S3. Relative expression of GhPME36 in WT and GhPME36-OE Arabidopsis (A) and cotton (B) plants. Fig. S4. Morphology and cell wall thickness of WT and GhPME36-KO line 3 cotton leaves. Fig. S5. DEGs identified via RNA-seq. Fig. S6. Extraction yield of CWM from the cotton leaves of three GhPME36-OE lines. Fig. S7. Soluble sugar content during different cotton leaf developmental stages. Fig. S8. Contents of monosaccharides and disaccharides in cotton leaves. Fig. S9. KEGG enrichment analysis of differentially accumulated metabolites and DEGs. Fig. S10. qPCR analysis of DEGs involved in flavonoid biosynthesis. Fig. S12. qPCR analysis of DEGs involved in phenylpropanoid biosynthesis. Fig. S12. qPCR analysis of DEGs involved in JA signal transduction. Fig. S13. Evolutionary tree of PMEIs created via the maximum likelihood method.

Additional file 2. Table S1. Indexing grade of cotton leaf damage following leaf miner infestation. Table S2. QC of transcriptome data. Table S3. DEGs encoding enzymes associated with cell wall polysaccharides. Table S4. KEGG enrichment of DEGs and metabolites. Table S5. Correlation between DEGs and metabolites (Ko00010). Table S6. DEGs related to flavonoid and phenylpropanoid biosynthesis. Table S7. Key DEGs related to JA signal transduction. Table S8. FPKM and *pl* values of five highly expressed GhPMEIs in cotton leaves. Table S9. Primers used in this study. Table S10. The individual data values for Fig. 1A, Fig. 2C-F, Fig. 3A-C, Fig. 4B-C, Fig. 5A, B, E, Fig. S1, Fig. S3A-B, Fig. S6-8, Fig. S10-12.

### Acknowledgements

We thank Prof. Zhi Wang (Institute of Cotton Research, Chinese Academy of Agricultural Sciences) for critical reading and editing of the manuscript and constructive suggestions. We are grateful for the computational resources supported by National Supercomputing Center in Zhengzhou and the guidance on sequencing analysis provided by Dr. Xu Gao (National

Supercomputing Center, Zhengzhou). We also wish to thank the anonymous peer reviewers for their valuable suggestions to improve the presentation of this research; we appreciate their comments and helpful suggestions.

### Authors' contributions

Z.Y., H.S., Y.Y., and M.W. conceived the project and designed the procedures. W.L., L.W., and S.W. created the transgenic plants. M.W., Z.Y., S.F., D.Z., T.L., J.H., and P.W. performed the experiments and analyzed the data. Z.Y. and M.W. wrote the manuscript. Z.Z., R.W., and M.D. provided technical assistance. All the authors read and approved the final manuscript.

### Funding

This work was funded by the Biological Breeding-Major Projects (2023ZD04062), the National Natural Science Foundation of China (32201828), Central Public-interest Scientific Institution Basal Research Fund (1610162023002), the National Agricultural Science and Technology Innovation Project for CAAS (CAAS-ASTIP-2016-ICR), the Science and Technologies R & D Program of Henan Province (232102111077), China Postdoctoral Science Foundation (2022M722899), and the State Key Laboratory of Cotton Biology Open Fund (CB2022A05).

### Availability of data and materials

Sequence information for *GhPME36* is deposited in the GenBank database under the accession number OP440573. The RNA-seq datasets generated from this study are deposited in the NCBI SRA under the accession number PRJNA884533. The individual data values of all experiments are presented in Additional file 2: Table S10.

### Declarations

#### Ethics approval and consent to participate

Not applicable.

#### Consent for publication

Not applicable.

#### Competing interests

The authors declare that they have no competing interests.

#### Author details

<sup>1</sup>Zhengzhou Research Base, National Key Laboratory of Cotton Bio-breeding and Integrated Utilization, School of Agricultural Sciences, Zhengzhou University, Zhengzhou 450001, China. <sup>2</sup>National Key Laboratory of Cotton Bio-breeding and Integrated Utilization, Institute of Cotton Research, Chinese Academy of Agricultural Sciences, Anyang 455000, China. <sup>3</sup>Hainan Seed Industry Laboratory, Sanya 572000, China. <sup>4</sup>Department of Environmental Sciences, Bahauddin Zakariya University, Multan, Pakistan. <sup>5</sup>Henan Grain and Cotton Crops Research Institute, Zhengzhou, China. <sup>6</sup>Shennong Laboratory, Zhengzhou 450002, China.

Received: 5 March 2024 Accepted: 29 August 2024

Published online: 11 September 2024

### References

- Xu L, Zhu L, Tu L, Liu L, Yuan D, Jin L, et al. Lignin metabolism has a central role in the resistance of cotton to the wilt fungus *Verticillium dahliae* as revealed by RNA-Seq-dependent transcriptional analysis and histochemistry. *J Exp Bot*. 2011;62(15):5607–21.
- Perlak FJ, Deaton RW, Armstrong TA, Fuchs RL, Sims SR, Greenplate JT, et al. Insect resistant cotton plants. *Biotechnology (N Y)*. 1990;8(10):939–43.
- Bragard C, Dehnen-Schmutz K, Di Serio F, Gonthier P, Jacques MA, Jacques Miret JA, et al. Pest categorisation of *Liriomyza sativae*. *Efsa j*. 2020;18(3): e06037.
- Oliveira JM, Araújo JL, Melo JWS, Dias-Pini NS. Melon genotypes with resistance to *Liriomyza sativae* Blanchard (Diptera: Agromyzidae). *Ann Acad Bras Cienc*. 2022;94(2): e20191244.

5. Nawaz R, Abbasi NA, Hafiz IA, Khan MF, Khalid A. Environmental variables influence the developmental stages of the citrus leafminer, infestation level and mined leaves physiological response of Kinnow mandarin. *Sci Rep*. 2021;11(1):7720.
6. Chang YW, Chen JY, Zheng SZ, Gao Y, Chen Y, Deng Y, et al. Revalidation of morphological characteristics and multiplex PCR for the identification of three congener invasive *Liriomyza* species (Diptera: Agromyzidae) in China. *PeerJ*. 2020;8: e10138.
7. Xu X, Coquilleau MP, Ridland PM, Umina PA, Yang Q, Hoffmann AA. Molecular identification of leafmining flies from Australia including new *Liriomyza* outbreaks. *J Econ Entomol*. 2021;114(5):1983–90.
8. Yule S, Htain NN, Oo AK, Sotelo-Cardona P, Srinivasan R. Occurrence of the South American tomato leaf miner, *Tuta absoluta* (Meyrick) in Southern Shan, Myanmar. *Insects*. 2021;12(11):962.
9. Pirtle EI, van Rooyen AR, Maino J, Weeks AR, Umina PA. A molecular method for biomonitoring of an exotic plant-pest: leafmining for environmental DNA. *Mol Ecol*. 2021;30(19):4913–25.
10. Dauphin BG, Ranocha P, Dunand C, Burlat V. Cell-wall microdomain remodeling controls crucial developmental processes. *Trends Plant Sci*. 2022;27(10):1033–48.
11. Chebli Y, Geitmann A. Cellular growth in plants requires regulation of cell wall biochemistry. *Curr Opin Cell Biol*. 2017;44:28–35.
12. Swaminathan S, Lionetti V, Zabolina OA. Plant cell wall integrity perturbations and priming for defense. *Plants (Basel)*. 2022;11(24):3539.
13. Bellincampi D, Cervone F, Lionetti V. Plant cell wall dynamics and wall-related susceptibility in plant-pathogen interactions. *Front Plant Sci*. 2014;5:228.
14. Vicré M, Lionetti V. Editorial: Plant cell wall in pathogenesis, parasitism and symbiosis, Volume II. *Front Plant Sci*. 2023;14:1230438.
15. Silva-Sanzana C, Celiz-Balboa J, Garzo E, Marcus SE, Parra-Rojas JP, Rojas B, et al. Pectin methylesterases modulate plant homogalacturonan status in defenses against the aphid *Myzus persicae*. *Plant Cell*. 2019;31(8):1913–29.
16. Gesteiro N, Butrón A, Estévez S, Santiago R. Unraveling the role of maize (*Zea mays* L.) cell-wall phenylpropanoids in stem-borer resistance. *Phytochemistry*. 2021;185:112683.
17. Wu HC, Huang YC, Stracovsky L, Jinn TL. Pectin methylesterase is required for guard cell function in response to heat. *Plant Signal Behav*. 2017;12(6): e1338227.
18. Jia H, Wang X, Wei T, Wang M, Liu X, Hua L, et al. Exogenous salicylic acid regulates cell wall polysaccharides synthesis and pectin methylation to reduce Cd accumulation of tomato. *Ecotoxicol Environ Saf*. 2021;207: 111550.
19. Somerville C, Bauer S, Brininstool G, Facette M, Hamann T, Milne J, et al. Toward a systems approach to understanding plant cell walls. *Science*. 2004;306(5705):2206–11.
20. Daher FB, Braybrook SA. How to let go: pectin and plant cell adhesion. *Front Plant Sci*. 2015;6:523.
21. Lionetti V, Fabri E, De Caroli M, Hansen AR, Willats WG, Piro G, et al. Three pectin methylesterase inhibitors protect cell wall integrity for *Arabidopsis* immunity to *Botrytis*. *Plant Physiol*. 2017;173(3):1844–63.
22. Mohnen D. Pectin structure and biosynthesis. *Curr Opin Plant Biol*. 2008;11(3):266–77.
23. Anderson CT. We be jammin': an update on pectin biosynthesis, trafficking and dynamics. *J Exp Bot*. 2016;67(2):495–502.
24. Wang T, Hong M. Solid-state NMR investigations of cellulose structure and interactions with matrix polysaccharides in plant primary cell walls. *J Exp Bot*. 2016;67(2):503–14.
25. Micheli F. Pectin methylesterases: cell wall enzymes with important roles in plant physiology. *Trends Plant Sci*. 2001;6(9):414–9.
26. Verbančić J, Lunn JE, Stitt M, Persson S. Carbon supply and the regulation of cell wall synthesis. *Mol Plant*. 2018;11(1):75–94.
27. Wang X, Wilson L, Cosgrove DJ. Pectin methylesterase selectively softens the onion epidermal wall yet reduces acid-induced creep. *J Exp Bot*. 2020;71(9):2629–40.
28. Soujanya PL, Sekhar JC, Ratnavathi CV, Karjagi CG, Shobha E, Suby SB, et al. Induction of cell wall phenolic monomers as part of direct defense response in maize to pink stem borer (*Sesamia inferens* Walker) and non-insect interactions. *Sci Rep*. 2021;11(1):14770.
29. Chebli Y, Kaneda M, Zerzour R, Geitmann A. The cell wall of the *Arabidopsis* pollen tube—spatial distribution, recycling, and network formation of polysaccharides. *Plant Physiol*. 2012;160(4):1940–55.
30. Bonnin E, Alvarado C, Crépeau MJ, Bouchet B, Garnier C, Jamme F, et al. Mobility of pectin methylesterase in pectin/cellulose gels is enhanced by the presence of cellulose and by its catalytic capacity. *Sci Rep*. 2019;9(1):12551.
31. Huang D, Mao Y, Guo G, Ni D, Chen L. Genome-wide identification of PME gene family and expression of candidate genes associated with aluminum tolerance in tea plant (*Camellia sinensis*). *BMC Plant Biol*. 2022;22(1):306.
32. Li Z, Wu L, Wang C, Wang Y, He L, Wang Z, et al. Characterization of pectin methylesterase gene family and its possible role in juice sac granulation in navel orange (*Citrus sinensis* Osbeck). *BMC Genomics*. 2022;23(1):185.
33. Li W, Shang H, Ge Q, Zou C, Cai J, Wang D, et al. Genome-wide identification, phylogeny, and expression analysis of pectin methylesterases reveal their major role in cotton fiber development. *BMC Genomics*. 2016;17(1):1000.
34. Cai J, Mo X, Wen C, Gao Z, Chen X, Xue C. FvMYB79 positively regulates strawberry fruit softening via transcriptional activation of FvPME38. *Int J Mol Sci*. 2021;23(1):101.
35. Yang W, Ruan M, Xiang M, Deng A, Du J, Xiao C. Overexpression of a pectin methylesterase gene PtoPME35 from *Populus tomentosa* influences stomatal function and drought tolerance in *Arabidopsis thaliana*. *Biochem Biophys Res Commun*. 2020;523(2):416–22.
36. Levesque-Tremblay G, Müller K, Mansfield SD, Haughn GW. HIGHLY METHYL ESTERIFIED SEEDS is a pectin methyl esterase involved in embryo development. *Plant Physiol*. 2015;167(3):725–37.
37. Yue X, Lin S, Yu Y, Huang L, Cao J. The putative pectin methylesterase gene, BcMF23a, is required for microspore development and pollen tube growth in *Brassica campestris*. *Plant Cell Rep*. 2018;37(7):1003–9.
38. Hongo S, Sato K, Yokoyama R, Nishitani K. Demethylesterification of the primary wall by PECTIN METHYLESTERASE35 provides mechanical support to the *Arabidopsis* stem. *Plant Cell*. 2012;24(6):2624–34.
39. Guénin S, Marek A, Rayon C, Lamour R, Assoumou Ndong Y, Domon JM, et al. Identification of pectin methylesterase 3 as a basic pectin methylesterase isoform involved in adventitious rooting in *Arabidopsis thaliana*. *New Phytol*. 2011;192(1):114–26.
40. Yan J, He H, Fang L, Zhang A. Pectin methylesterase31 positively regulates salt stress tolerance in *Arabidopsis*. *Biochem Biophys Res Commun*. 2018;496(2):497–501.
41. Reem NT, Chambers L, Zhang N, Abdullah SF, Chen Y, Feng G, et al. Post-synthetic reduction of pectin methylesterification causes morphological abnormalities and alterations to stress response in *Arabidopsis thaliana*. *Plants (Basel)*. 2020;9(11):1558.
42. Roig-Oliver M, Rayon C, Roulard R, Fourné F, Bota J, Flexa J. Reduced photosynthesis in *Arabidopsis thaliana* atpme17.2 and atpae11.1 mutants is associated to altered cell wall composition. *Physiol Plant*. 2021;172(3):1439–51.
43. Coculo D, Lionetti V. The plant invertase/pectin methylesterase inhibitor superfamily. *Front Plant Sci*. 2022;13: 863892.
44. Di Matteo A, Giovane A, Raiola A, Camardella L, Bonivento D, De Lorenzo G, et al. Structural basis for the interaction between pectin methylesterase and a specific inhibitor protein. *Plant Cell*. 2005;17(3):849–58.
45. Wormit A, Usadel B. The multifaceted role of pectin methylesterase inhibitors (PMEIs). *Int J Mol Sci*. 2018;19(10):2878.
46. Lionetti V, Cervone F, Bellincampi D. Methyl esterification of pectin plays a role during plant-pathogen interactions and affects plant resistance to diseases. *J Plant Physiol*. 2012;169(16):1623–30.
47. Coculo D, Del Corpo D, Martínez MO, Vera P, Piro G, De Caroli M, et al. *Arabidopsis* subtilases promote defense-related pectin methylesterase activity and robust immune responses to *botrytis* infection. *Plant Physiol Biochem*. 2023;201: 107865.
48. Lionetti V, Raiola A, Camardella L, Giovane A, Obel N, Pauly M, et al. Overexpression of pectin methylesterase inhibitors in *Arabidopsis* restricts fungal infection by *Botrytis cinerea*. *Plant Physiol*. 2007;143(4):1871–80.
49. Osorio S, Castillejo C, Quesada MA, Medina-Escobar N, Brownsey GJ, Suau R, et al. Partial demethylation of oligogalacturonides by pectin methylesterase 1 is required for eliciting defence responses in wild strawberry (*Fragaria vesca*). *Plant J*. 2008;54(1):43–55.

50. Komarova TV, Sheshukova EV, Dorokhov YL. Cell wall methanol as a signal in plant immunity. *Front Plant Sci.* 2014;5:101.
51. Li M, Liu M, Peng F, Fang L. Influence factors and gene expression patterns during MeJa-induced gummosis in peach. *J Plant Physiol.* 2015;182:49–61.
52. Madsen NEL, Sørensen PB, Offenberg J. Sugar and amino acid preference in the black garden ant *Lasius niger* (L.). *J Insect Physiol.* 2017;100:140–5.
53. Broadhead GT, Raguso RA. Associative learning of non-sugar nectar components: amino acids modify nectar preference in a hawkmoth. *J Exp Biol.* 2021;224(12):jeb234633.
54. Koes R, Verweij W, Quattrocchio F. Flavonoids: a colorful model for the regulation and evolution of biochemical pathways. *Trends Plant Sci.* 2005;10(5):236–42.
55. Shen Y, Sun T, Pan Q, Anupol N, Chen H, Shi J, et al. RrMYB5- and RrMYB10-regulated flavonoid biosynthesis plays a pivotal role in feedback loop responding to wounding and oxidation in *Rosa rugosa*. *Plant Biotechnol J.* 2019;17(11):2078–95.
56. Dong NQ, Lin HX. Contribution of phenylpropanoid metabolism to plant development and plant-environment interactions. *J Integr Plant Biol.* 2021;63(1):180–209.
57. Ruan J, Zhou Y, Zhou M, Yan J, Khurshid M, Weng W, et al. Jasmonic acid signaling pathway in plants. *Int J Mol Sci.* 2019;20(10):2479.
58. Del Corpo D, Fullone MR, Miele R, Lafond M, Pontiggia D, Grisel S, et al. AtPME17 is a functional *Arabidopsis thaliana* pectin methylesterase regulated by its PRO region that triggers PME activity in the resistance to *Botrytis cinerea*. *Mol Plant Pathol.* 2020;21(12):1620–33.
59. Del Corpo D, Coculo D, Greco M, De Lorenzo G, Lionetti V. Pull the fuzes: Processing protein precursors to generate apoptotic danger signals for triggering plant immunity. *Plant Commun.* 2024;5(8): 100931.
60. Zhang T, Hu Y, Jiang W, Fang L, Guan X, Chen J, et al. Sequencing of allo-tetraploid cotton (*Gossypium hirsutum* L. acc. TM-1) provides a resource for fiber improvement. *Nat Biotechnol.* 2015;33(5):531–7.
61. Wilkins TA, Arpat AB. The cotton fiber transcriptome. *Physiol Plant.* 2005;124(3):295–300.
62. Huang YC, Wu HC, Wang YD, Liu CH, Lin CC, Luo DL, et al. PECTIN METHYLESTERASE34 contributes to heat tolerance through its role in promoting stomatal movement. *Plant Physiol.* 2017;174(2):748–63.
63. Wen F, Zhu Y, Hawes MC. Effect of pectin methylesterase gene expression on pea root development. *Plant Cell.* 1999;11(6):1129–40.
64. Liu N, Sun Y, Pei Y, Zhang X, Wang P, Li X, et al. A pectin methylesterase inhibitor enhances resistance to *Verticillium* wilt. *Plant Physiol.* 2018;176(3):2202–20.
65. Wang M, Yuan D, Gao W, Li Y, Tan J, Zhang X. A comparative genome analysis of PME and PME1 families reveals the evolution of pectin metabolism in plant cell walls. *PLoS ONE.* 2013;8(8): e72082.
66. Hothorn M, Wolf S, Aloy P, Greiner S, Scheffzek K. Structural insights into the target specificity of plant invertase and pectin methylesterase inhibitory proteins. *Plant Cell.* 2004;16(12):3437–47.
67. An SH, Sohn KH, Choi HW, Hwang IS, Lee SC, Hwang BK. Pepper pectin methylesterase inhibitor protein CaPMEI1 is required for antifungal activity, basal disease resistance and abiotic stress tolerance. *Planta.* 2008;228(1):61–78.
68. Vincent RR, Williams MA. Microrheological investigations give insights into the microstructure and functionality of pectin gels. *Carbohydr Res.* 2009;344(14):1863–71.
69. Parre E, Geitmann A. Pectin and the role of the physical properties of the cell wall in pollen tube growth of *Solanum chacoense*. *Planta.* 2005;220(4):582–92.
70. Bethke G, Grundman RE, Sreekanta S, Truman W, Katagiri F, Glazebrook J. *Arabidopsis* PECTIN METHYLESTERASEs contribute to immunity against *Pseudomonas syringae*. *Plant Physiol.* 2014;164(2):1093–107.
71. Hewezi T, Howe P, Maier TR, Hussey RS, Mitchum MG, Davis EL, et al. Cellulose binding protein from the parasitic nematode *Heterodera schachtii* interacts with *Arabidopsis* pectin methylesterase: cooperative cell wall modification during parasitism. *Plant Cell.* 2008;20(11):3080–93.
72. Raiola A, Lionetti V, Elmaghraby I, Immerzeel P, Mellerowicz EJ, Salvi G, et al. Pectin methylesterase is induced in *Arabidopsis* upon infection and is necessary for a successful colonization by necrotrophic pathogens. *Mol Plant Microbe Interact.* 2011;24(4):432–40.
73. Dai X, You M, Fu L. The influences of water-soluble substances from other plants on the host-selection of *Liriomyza sativae*. *Journal of Fujian Agricultural University.* 2001;30(4):490–2.
74. Livak KJ, Schmittgen TD. Analysis of relative gene expression data using real-time quantitative PCR and the 2<sup>-</sup>(Delta Delta C(T)) Method. *Methods.* 2001;25(4):402–8.
75. Zhang B. *Agrobacterium*-mediated genetic transformation of cotton. *Methods Mol Biol.* 2019;1902:19–33.
76. Clough SJ, Bent AF. Floral dip: a simplified method for *Agrobacterium*-mediated transformation of *Arabidopsis thaliana*. *Plant J.* 1998;16(6):735–43.
77. Hagerman AE, Austin PJ. Continuous spectrophotometric assay for plant pectin methyl esterase. *J Agric Food Chem.* 1986;34(3):440–4.
78. Luo Z-M, Wang X-Y, Huang Y-K, Zhang R-Y, Li W-F, Shan H-L, et al. Field resistance of different sugarcane varieties to sugarcane thrips (*Fulmekiola serratus*) in China. *Sugar Tech.* 2019;21(3):527–31.
79. Vitha S, Osteryoung KW. Immunofluorescence microscopy for localization of *Arabidopsis* chloroplast proteins. *Methods Mol Biol.* 2011;774:33–58.
80. Perteau M, Perteau GM, Antonescu CM, Chang TC, Mendell JT, Salzberg SL. StringTie enables improved reconstruction of a transcriptome from RNA-seq reads. *Nat Biotechnol.* 2015;33(3):290–5.
81. Love MI, Huber W, Anders S. Moderated estimation of fold change and dispersion for RNA-seq data with DESeq2. *Genome Biol.* 2014;15(12):550.

## Publisher's Note

Springer Nature remains neutral with regard to jurisdictional claims in published maps and institutional affiliations.